



CrossMark  
click for updates

Cite this: *Chem. Sci.*, 2015, 6, 4451

# Tricyclic analogues of epidithiodioxopiperazine alkaloids with promising *in vitro* and *in vivo* antitumor activity†

Marcus Baumann,<sup>a</sup> André P. Dieskau,<sup>a</sup> Brad M. Loertscher,<sup>a</sup> Mary C. Walton,<sup>a</sup> Sangkil Nam,<sup>b</sup> Jun Xie,<sup>b</sup> David Horne<sup>\*b</sup> and Larry E. Overman<sup>\*a</sup>

Epipolythiodioxopiperazine (ETP) alkaloids are structurally elaborate alkaloids that show potent antitumor activity. However, their high toxicity and demonstrated interactions with various biological receptors compromises their therapeutic potential. In an effort to mitigate these disadvantages, a short stereocontrolled construction of tricyclic analogues of epidithiodioxopiperazine alkaloids was developed. Evaluation of a small library of such structures against two invasive cancer cell lines defined initial structure–activity relationships (SAR), which identified 1,4-dioxohexahydro-6*H*-3,8*a*-epidithiopyrrolo[1,2-*a*]pyrazine **3c** and related structures as particularly promising antitumor agents. ETP alkaloid analogue **3c** exhibits low nanomolar activity against both solid and blood tumors *in vitro*. In addition, **3c** significantly suppresses tumor growth in mouse xenograft models of melanoma and lung cancer, without obvious signs of toxicity, following either intraperitoneal (IP) or oral administration. The short synthesis of molecules in this series will enable future mechanistic and translational studies of these structurally novel and highly promising clinical antitumor candidates.

Received 27th April 2015

Accepted 26th May 2015

DOI: 10.1039/c5sc01536g

www.rsc.org/chemicalscience

## Introduction

Epipolythiodioxopiperazines (ETPs) constitute a group of structurally complex and biologically active fungal alkaloids that are characterized structurally by a transannular polysulfide unit joining carbons 3 and 6 of their 2,5-dioxopiperazine rings (Fig. 1). A broad spectrum of biological activities is associated with this family of natural products.<sup>1</sup> Two commercially available members of this group, chaetomin (**1**) and chaetocin A (**2**), have received extensive study. Early on, chaetomin was identified as an inhibitor of HIF-1 transcriptional activity, although its toxicity prevented its further development for cancer therapy.<sup>2</sup> Chaetocin A continues to be actively investigated as a potential cancer therapeutic, with good activity registered *in vitro*<sup>1,3</sup> and in animal models<sup>1,3d,4</sup> against blood and solid tumors. A number of molecular targets of chaetocin A have been identified, and various mechanisms contributing to its cytotoxicity are now recognized.<sup>3b–e,5</sup> Recently, several structurally simple analogues

of ETP alkaloids have been prepared and their *in vitro* cytotoxicity registered against a few cancer cell lines.<sup>6</sup>

The high cytotoxicity of ETP alkaloids **1** and **2**,<sup>2,5a</sup> and their promiscuous interactions with biological receptors, renders these natural products unattractive candidates for further development as anticancer agents. Nonetheless, we anticipated that less toxic and more selective antitumor agents could be found by significantly simplifying the structure of these alkaloids. As good *in vitro* cytotoxicity against several cancer cell lines is maintained in natural product analogues of

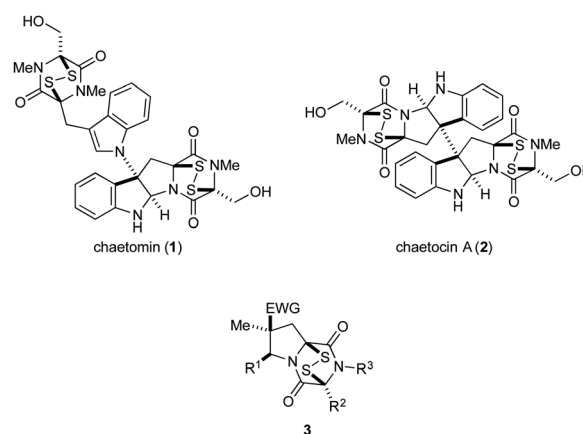


Fig. 1 Two ETP alkaloids and structurally simplified tricyclic analogues **3**.

<sup>a</sup>Department of Chemistry, 1102 Natural Sciences II, University of California, Irvine, California 92697-2025, USA. E-mail: leoverma@uci.edu

<sup>b</sup>Department of Molecular Medicine, Beckman Research Institute of City Hope Comprehensive Cancer Center, 1500 E. Duarte Road, Duarte, California 91010, USA. E-mail: dhorne@cih.org

† Electronic supplementary information (ESI) available: Table summarizing yields and diastereoselectivity in the synthesis of ETP alkaloid analogues **3**, experimental procedures, and characterization data for all new compounds. CCDC 1061869–1061873. For ESI and crystallographic data in CIF or other electronic format see DOI: 10.1039/c5sc01536g



chaetocin A that contain a single ETP fragment,<sup>6b-d</sup> we investigated 1,4-dioxohexahydro-6H-3,8a-epidithiopyrrolo[1,2-a]pyrazines **3**, analogues of chaetomin and chaetocin A that retain only three of the natural products' nine or ten rings.<sup>7</sup>

We report herein an expeditious synthesis of analogues **3** that allows easy introduction of substituents at four sites. The *in vitro* antitumor activity of 19 molecules in this series was evaluated against invasive human prostate cancer and melanoma cell lines. IC<sub>50</sub> values of **3c**, the most potent compound in this series, were determined using nine additional cancer cell lines, and **3c** was evaluated also in xenograft tumor models of human lung cancer and melanoma.

## Results and discussion

### Synthesis of ETP analogues **3**

The general scheme used to prepare a library of 1,4-dioxohexahydro-6H-3,8a-epidithiopyrrolo[1,2-a]pyrazines **3** is outlined in Scheme 1. As the building blocks **4**, **6**, and **7** can be varied widely, a diversity of structures is readily prepared, most by way of only two isolated and purified intermediates (pyrrolidine **5** and dioxopiperazine **8**).

The synthesis begins with 1,3-dipolar cycloaddition of azomethine ylides generated *in situ* by 1,2-protopropic shifts of glycine imines with  $\alpha$ -methyl-substituted dipolarophiles in the presence of LiBr and Et<sub>3</sub>N.<sup>8,9</sup> It was found that imine formation was most efficient in acetonitrile, whereas the cycloaddition was cleanest in THF. In general, this two-step process delivered the desired pyrrolidine products in useful yields (45–85%) and high purity on multi-gram scales. As expected, this cycloaddition took place with high *endo* stereoselectivity (>10 : 1) when methyl methacrylate was employed as the dipolarophile. Cycloadditions employing methacrylonitrile took place with lower *endo* stereoselectivity, which varied considerably with the nature of the R<sup>1</sup> substituent (see Table 1 of the ESI†). In some cases, the major *endo* cycloadduct **5** could be separated in good yield from the cycloadduct mixture by its lower solubility in 1 : 1 MeOH/CH<sub>2</sub>Cl<sub>2</sub>, although generally higher yields of this adduct were realized by purification of the crude product by flash chromatography on silica gel.

The relative configuration of the cycloadducts in the nitrile series was assigned on the basis of their distinctive <sup>1</sup>H NMR chemical shifts (Fig. 2). In the *exo* cycloadducts, the C4 methyl

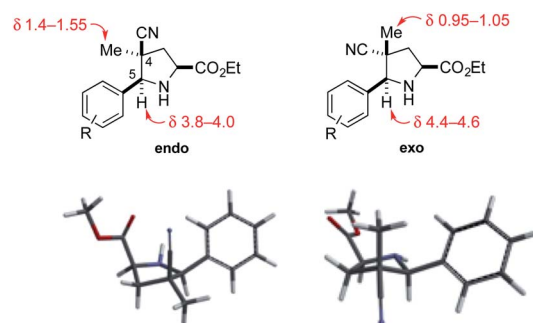
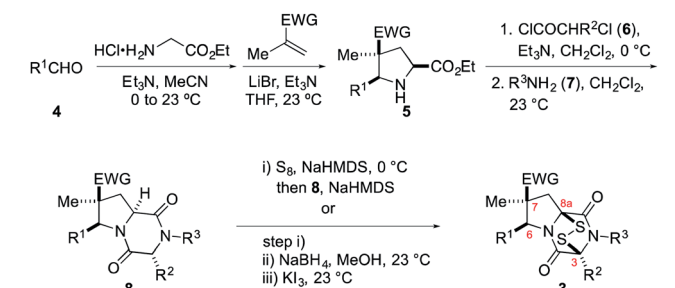


Fig. 2 *Endo* and *exo* pyrrolidine cycloadducts: diagnostic <sup>1</sup>H NMR signals (in CDCl<sub>3</sub>) and models of their low-energy conformations.

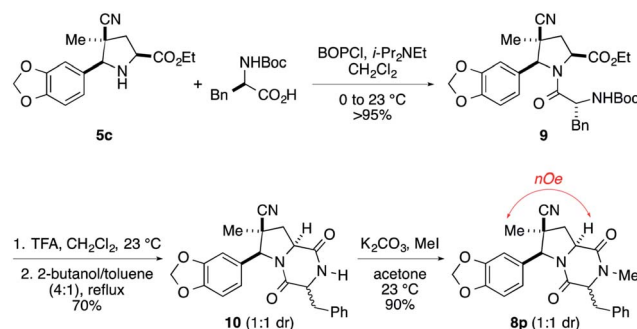
substituent was observed at a diagnostic upfield chemical shift ( $\delta$  0.95–1.05 ppm), consistent with its position within the shielding cone of the C5 aryl substituent. The chemical shift of the C5 benzylic methine hydrogen was also diagnostic, appearing upfield by  $\sim$ 0.6 ppm in the *endo* cycloadduct.

Cycloadducts **5** could be elaborated to dioxopiperazines **8** in a number of standard ways.<sup>10</sup> A convenient sequence is depicted in Scheme 1 whereby the amino ester **5** was first acylated with 2-chloropropionyl chloride (**6**, R<sup>2</sup> = Me) and the crude  $\alpha$ -chloroamide intermediate was coupled with a primary amine **7** to form the dioxopiperazine product. For example, the formation of dioxopiperazines **8** having R<sup>3</sup> = Me was accomplished by stirring a biphasic mixture of the crude  $\alpha$ -chloroamide in CH<sub>2</sub>Cl<sub>2</sub> with 40% aqueous methylamine at room temperature for 12–16 h. In most cases, the dioxopiperazine intermediate was isolated as a crystalline solid without the need for chromatographic purification. This solid was either a single stereoisomer or a mixture of C3 epimers. In two cases, the relative configuration of the major stereoisomer was confirmed by single-crystal X-ray analysis.<sup>11</sup>

An alternate sequence that allows ready incorporation of a variety of R<sup>2</sup> substituents for the synthesis of dioxopiperazine **8p** having R<sup>2</sup> = Bn is illustrated in Scheme 2. Coupling of cycloadduct **5c** with *N*-Boc-phenylalanine using BOPCl gave dipeptide **9** in high yield. Standard removal of the Boc group followed by heating the product in refluxing 2-butanol/toluene (4 : 1) gave dioxopiperazine **10** in 70% yield as a 1 : 1 mixture of stereoisomers. After these products were separated on silica gel,



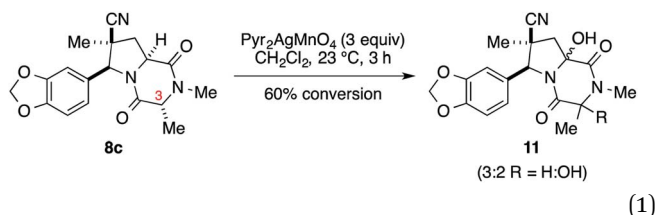
Scheme 1 Synthesis of ETP alkaloid analogues **3** (EWG = CO<sub>2</sub>Me or CN).



Scheme 2 An alternate route to dioxopiperazine intermediates.

they were individually *N*-methylated in high yield upon reaction with MeI and K<sub>2</sub>CO<sub>3</sub>. That products **8p** were epimers at the benzyl stereocenter was established by strong <sup>1</sup>H NOEs between the quaternary methyl substituent and the angular methine hydrogen.

We initially examined elaboration of dioxopiperazine **8c** to the corresponding ETP derivatives by attempting to first selectively oxidize the methine hydrogens of the dioxopiperazine ring. The most successful of the oxidants screened was Pyr<sub>2</sub>-AgMnO<sub>4</sub>, which had been employed with great success by Movassaghi for this purpose.<sup>12</sup> This reagent cleanly hydroxylated the angular carbon; however, under the conditions we examined, hydroxylation at C3 did not proceed to full conversion before decomposition of the diol product became problematic (eqn (1)).<sup>‡</sup>



We turned to introduce the epidisulfide unit by base-promoted disulfenylation of the dioxopiperazine intermediates.<sup>13</sup> In initial studies, dioxopiperazines **8** were converted to the corresponding ETP derivatives by the general procedure introduced by Nicolaou and coworkers.<sup>14</sup> After purification by flash chromatography or preparative TLC, ETP products **3** were obtained in low to moderate yields (generally 20–30%, Scheme 1). During attempts to optimize this sequence, we discovered that the desired disulfide **3**, typically contaminated with 5–20% of the corresponding trisulfide, was the predominant sulfur-containing product produced after the sulfenylation step. This result stands in contrast to the formation of largely the tetrasulfide intermediate in the base-promoted sulfenylation of nearly flat dioxopiperazines.<sup>15</sup> As the epidithiodioxopiperazine products **3** could be separated from their trisulfide analogues by flash chromatography or preparative TLC, this operationally simple one-step procedure was generally used in our studies giving **3** in 6–46% yield (see Table 1 of the ESI†).

Stereoisomer **3** having the disulfide bridge on the same face as the nitrile and aryl substituents was typically produced with 5–10 : 1 diastereoselectivity. In two cases (**3c** and **3e**), this product was characterized by single-crystal X-ray analysis.<sup>11</sup> Epidisulfide stereoisomer **3e** and diastereomer **12** having the disulfide bridge on the opposite face of the dioxopiperazine are easily distinguished by <sup>1</sup>H NMR analysis. Particularly diagnostic are the chemical shifts of the C7 methylene hydrogens H<sub>A</sub> (*syn* to CN) and H<sub>B</sub> (*anti* to CN).<sup>§</sup> As illustrated in Fig. 3 for **3e** and **12**, these diastereotopic hydrogens are observed at similar chemical shift in the major stereoisomer **3e**, whereas in diastereomer **12** the chemical shifts of these hydrogens differ by 1.3 ppm, with H<sub>A</sub> being observed at  $\delta$  3.84 and H<sub>B</sub> at  $\delta$  2.53. The observation of the C7 methylene hydrogens at similar chemical shift ( $\Delta\delta$  0.3–

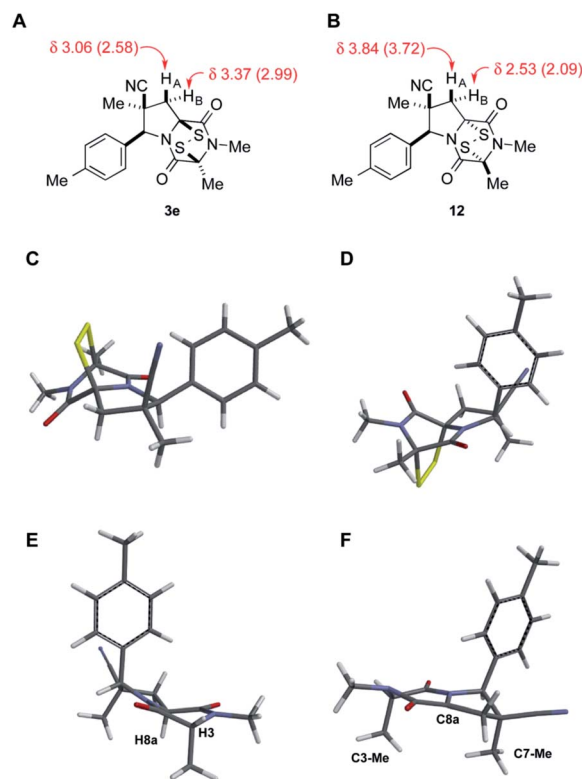


Fig. 3 Representative data used to assign the relative configuration of the disulfide bridge in ETP products, X-ray model of dioxopiperazine **8e**, and a computation model of the derived angular enolate. (A and B) show the observed (in CDCl<sub>3</sub>) and calculated (in parentheses) chemical signals of the methylene hydrogens of the pyrrolidine ring of ETP diastereomers **3e** and **12**. (C) is the X-ray model of **3e**. (D) is the computational model (B3LYP/631-G\*) of **12**. (E) is the X-ray model of dioxopiperazine **8e**. (F) is the predominant conformer (B3LYP/631-G\*) of the angular enolate formed from dioxopiperazine **8e**.

0.4 ppm) was seen also in <sup>1</sup>H NMR spectra of crystallographically characterized **3c**, and this trend in chemical shift was used to assign the relative configuration to other ETP products **3** prepared in this study. In cases where the epidisulfide diastereomer was isolated and characterized, the chemical shift difference between its methylene hydrogens ranged from 1.1–1.4 ppm (see the ESI†). Using the X-ray model of **3e** and a computational model (B3LYP/631-G\*) of diastereomer **12**, the chemical shifts (shown in parentheses in Fig. 3A and B) of the C7 methylene hydrogens of the two ETP stereoisomers were calculated and found to be in accord with the observed trend.¶

The origin of diastereoselection in the preferential formation of epidisulfide stereoisomer **3** is poorly understood at this time. We hypothesize that enolization and subsequent configuration-determining sulfenylation occurs initially at the angular C8a carbon, because the expected boat conformation of the dioxopiperazine precursor positions the C3 methine hydrogen nearly coplanar with the adjacent carbonyl group (see X-ray model Fig. 3E).<sup>11</sup> Consistent with this suggestion, treatment of dioxopiperazine **8e** with 0.5, 1.0 and 1.5 equiv. of NaHMDS at room temperature, followed by quenching with D<sub>2</sub>O after 10 min resulted in preferential deuteration at C8a. The predominant

conformer of the C8a enolate of **8e** found by computational modeling is depicted in Fig. 3F. Sulfenylation at C8a from the bottom face (*anti* to CN) of this enolate would be disfavored by the “axially” oriented methyl groups at C3 and C7, whereas sulfenylation from the top face would be disfavored by the orientation of the *p*-tolyl substituent. Perhaps the potential of the *p*-tolyl substituent to minimize its steric influence by a 30–40° rotation about the aryl carbon–C6  $\sigma$ -bond is responsible for the observed facial selectivity in forming the disulfide bridge.

A summary of the ETP alkaloid analogues prepared during this investigation and the yields obtained for each of the three steps is provided in Table 1 of the ESI.† Purification by chromatography was only necessary after the 1,3-dipolar cycloaddition and disulfenylation steps, whereas purification of the 2,6-dioxopiperazines was accomplished by trituration in most cases.

### Antitumor activity

With a selection of ETP alkaloid analogues in hand, their *in vitro* cytotoxicity against two highly invasive cancer cell lines, DU145 (human prostate cancer) and A2058 (human melanoma) were determined (Table 1). Analogues **3a** and **3b**, in which the electron-withdrawing substituent in the pyrrolidine ring is a methyl ester, exhibited no observable activity ( $IC_{50}$  values  $> 5 \mu M$ ). In contrast, the corresponding analogues incorporating a nitrile are considerably more cytotoxic, particularly in the methylenedioxyphenyl series as shown by comparison of **3b** and **3c**. Of the molecules in this series explored to date, **3c** is the most potent showing  $IC_{50}$  values against DU145 and A2058 tumor cells in the double-digit nanomolar range that are comparable to those found for chaetocin A (**2**) under identical assay conditions.<sup>6d</sup> The presence of oxygen at *meta* and *para* positions of the aryl substituent is beneficial, with the absence of oxygen at the *meta* position (**3g**), at the *para* position (**3k**), or at both the *meta* and *para* positions (**3f** and **3j**) resulting in a 4–15-fold reduction in cytotoxicity. When the electron-donating groups at C3 and C4 are replaced by weaker donors, cytotoxicity is reduced (compare **3g** with **3h**, and **3c** with **3i**). A small alkyl substituent on the nitrogen atom of dioxopiperazine ring is favored, with an *n*-Bu or morpholinoethyl substituent reducing cytotoxicity by an order of magnitude (compare **3c**, **3m**, and **3o**). However, substituting methyl for ethyl (**3l**) or cyclopropyl (**3n**) at this position has only minimal effect on cytotoxicity. Methyl is favored over benzyl at the sulfur-bearing carbon of the dioxopiperazine ring, although the significant activity of benzyl analogue **3p** suggests that substitution is tolerated at this site.

It was particularly important to establish that relative and absolute configuration of the early lead compound **3c** is important for activity. Analogue **13**, having the opposite relative configuration of the disulfide bridge to **3c**, showed decreased potency against DU145 and A2058. Analogues **14** and **15**, which are derived from the minor *exo* cycloadduct *epi-5c*, and, thus, have the nitrile substituent *trans* to the aryl substituent, showed weak activity only. We were able to separate the two enantiomers of **3c** by enantioselective chromatography and assign their absolute configurations by a combination of CD analysis and

**Table 1** Activity of ETP alkaloid analogues **3** against human prostate cancer (DU145) and melanoma (A2058) cell lines

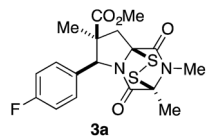
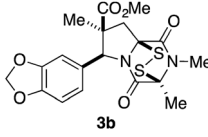
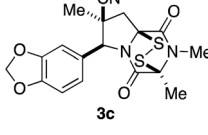
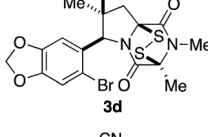
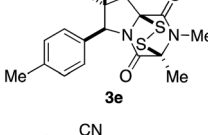
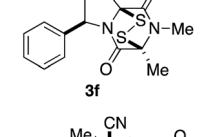
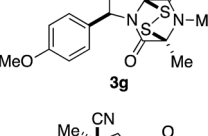
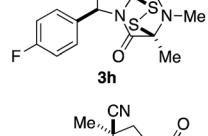
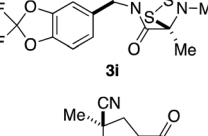
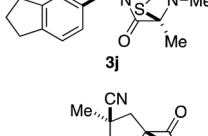
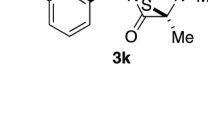
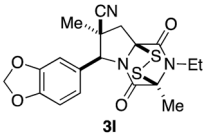
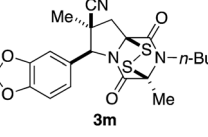
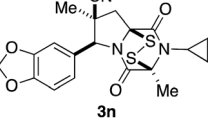
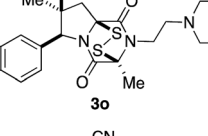
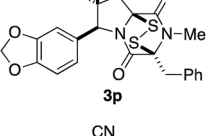
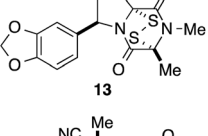
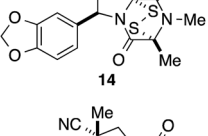
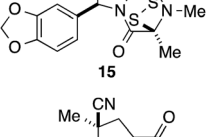
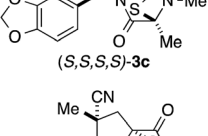
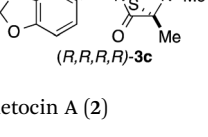
| Compound  | $IC_{50}$ ( $\mu M$ ) |                  |
|---|-----------------------|------------------|
|   | DU145 (prostate)      | A2058 (melanoma) |
| <br><b>3a</b>   | >5                    | >5               |
| <br><b>3b</b>   | >5                    | >5               |
| <br><b>3c</b>   | 0.10                  | 0.06             |
| <br><b>3d</b>   | 0.26                  | 0.24             |
| <br><b>3e</b>  | 0.59                  | 0.50             |
| <br><b>3f</b> | 0.78                  | 0.87             |
| <br><b>3g</b> | 0.42                  | 0.65             |
| <br><b>3h</b> | 2.0                   | 1.6              |
| <br><b>3i</b> | 0.71                  | 0.42             |
| <br><b>3j</b> | 0.75                  | 0.50             |
| <br><b>3k</b> | 0.92                  | 0.50             |





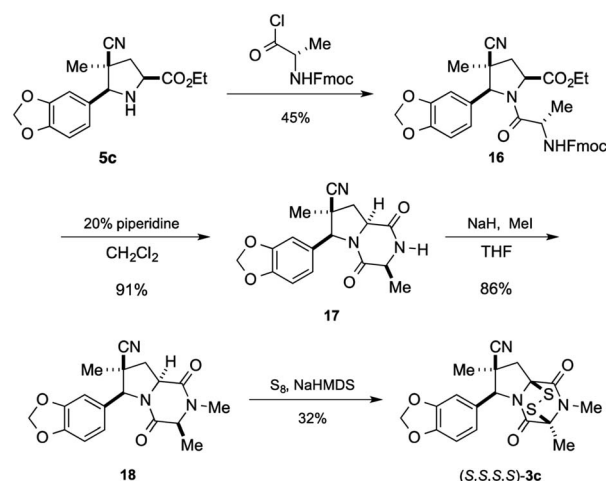
Table 1 (Contd.)

| Compound   | IC <sub>50</sub> (μM) |                  |
|--|-----------------------|------------------|
|  | DU145 (prostate)      | A2058 (melanoma) |
| <br><b>3l</b>             | 0.24                  | 0.10             |
| <br><b>3m</b>             | 1.2                   | 0.82             |
| <br><b>3n</b>             | 0.26                  | 0.07             |
| <br><b>3o</b>             | 0.90                  | 0.61             |
| <br><b>3p</b>            | 0.31                  | 0.35             |
| <br><b>13</b>           | 0.75                  | 0.22             |
| <br><b>14</b>           | 2.2                   | 3.8              |
| <br><b>15</b>           | 0.87                  | 0.51             |
| <br><b>(S,S,S,S)-3c</b> | 0.13                  | 0.06             |
| <br><b>(R,R,R,R)-3c</b> | 0.81                  | 0.75             |
| Chaetocin A ( <b>2</b> )   | 0.073                 | 0.061            |

single-crystal X-ray crystallography. The (*S,S,S,S*)-enantiomer of **3c** (the absolute configuration depicted for all racemic ETP alkaloid analogues in this report) was found to be more active by a factor of five against DU145 cells and a factor of ten against A2058 cells compared to the (*R,R,R,R*)-enantiomer of **3c**.

Having established that the (*S,S,S,S*)-enantiomer was the more active form of **3c**, we developed a method to access it selectively. This was achieved by acylation of racemic pyrrolidine **5c** with Fmoc-L-alanyl chloride and chromatographic separation of the diastereoisomeric products to afford enantiopure amide **16** in 45% yield (Scheme 3).<sup>\*\*</sup> Cleavage of the Fmoc group lead to spontaneous formation of 2,6-dioxopiperazine **17** and subsequent *N*-methylation furnished **18**. Disulfenylation of **18** proceeded in modest yield to afford enantiopure (*S,S,S,S*)-**3c**.

The lead compound in this series, ( $\pm$ )-**3c**, was screened against eleven cancer cell lines representing eight cancer types (Table 2). Low single-digit nanomolar activity was observed for both solid (Huh-7 liver) and blood (AML) cancers. In addition, analogue ( $\pm$ )-**3c** was shown to significantly suppress tumor growth in xenograft tumor models of melanoma (Fig. 4A) and lung cancer (Fig. 4B) by intraperitoneal (IP) injection or oral

Scheme 3 Synthesis of (*S,S,S,S*)-**3c**.Table 2 Activity of ( $\pm$ )-**3c** against eleven cancer cell lines

| Cancer type | Cell line | IC <sub>50</sub> (nM) |
|-------------|-----------|-----------------------|
| Prostate    | DU145     | 130                   |
| Melanoma    | A2058     | 100                   |
| Ovarian     | SKOV3     | 90                    |
| Breast      | HCC38     | 75                    |
| AML         | MV4-11    | 1.8                   |
| Lung        | A549      | 100                   |
| Liver       | Huh-7     | 3.3                   |
|             | HepG2     | 14                    |
| Pancreatic  | SU.86.86  | 86                    |
|             | BxPC3     | 210                   |
|             | Panc1     | 824                   |



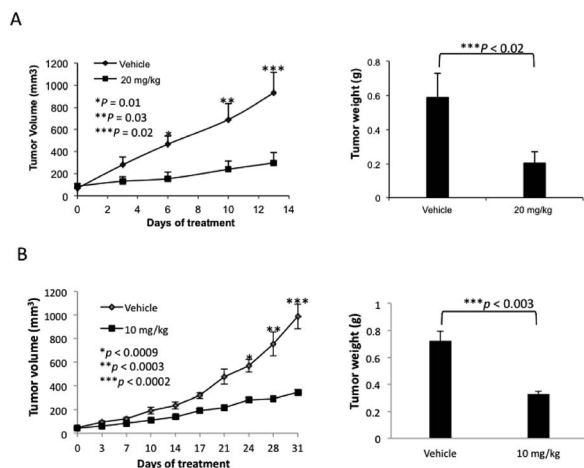


**Fig. 4** Agent (±)-**3c** suppresses tumor growth in xenografts of A2058 human melanoma (A) and A549 human non-small lung cancer cells (B). (A) A2058 human melanoma cells ( $3 \times 10^6$ ) were subcutaneously injected into the flanks of 5–6 weeks old athymic female nude mice. When palpable tumor sizes reached approximately 100 mm<sup>3</sup>, (±)-**3c** was administered by IP injection at 20 mg kg<sup>−1</sup> once daily for 13 days. (B) A549 human non-small lung cancer cells ( $5 \times 10^6$ ) were subcutaneously injected into the flanks of 5–6 weeks old female NSG mice. When palpable tumor sizes reached approximately 50 mm<sup>3</sup>, (±)-**3c** was orally administered at 10 mg kg<sup>−1</sup> once daily for 31 days.

administration. Consistent with suppression of tumor volumes, analogue (±)-**3c** slowed growth of tumor weights in both mouse xenograft models. In addition, no obvious signs of toxicity (e.g., weight loss or diarrhea) were observed in the mice during these studies.

## Conclusion

A short sequence, typically involving the isolation and purification of only two intermediates, was developed for preparing 1,4-dioxohexahydro-6*H*-3,8a-epidithiopyrrolo[1,2-*a*]pyrazines **3**. The sequence begins with the *endo*-stereoselective dipolar cycloaddition of glycine imines of aryl aldehydes with methyl methacrylate or methacrylonitrile. The pyrrolidine ester products **5** are converted in standard ways to dioxopiperazines **8**, which are transformed with modest stereoselectivity to ETP alkaloid analogues **3** by reaction with NaHMDS and S<sub>8</sub>. In contrast to other applications of this procedure for sulfonylation,<sup>15</sup> episulfide products are formed predominantly in this step.

The racemic 1,4-dioxohexahydro-6*H*-3,8a-epidithiopyrrolo[1,2-*a*]pyrazines **3** prepared in this study, which are analogues of polycyclic ETP alkaloids such as chaetomin (**1**) and chaetocin A (**2**), were screened initially against two invasive human cancer cell lines: DU145 (prostate cancer) and A2058 (melanoma). Most of these analogues showed IC<sub>50</sub> values of <1 μM. The highest cytotoxicity against these cell lines was seen with analogues **3** containing a nitrile substituent, an electron-rich aromatic ring, and two methyl substituents in the dioxopiperazine ring, with analogue **3c** emerging as the lead compound in this series. Stereoisomers of **3c** (**13**, **14**, and **15**) showed reduced activity,

and separation of the enantiomers of **3c** demonstrated that cytotoxicity resided largely in the (*S,S,S,S*)-enantiomer. In screening against an additional nine cancer cell lines, analogue (±)-**3c** showed low single-digit nanomolar activity against both blood (AML) and solid (Huh-7 liver) cancers. Of particular significance, analogue (±)-**3c** showed promising *in vivo* activity in xenograft models of human melanoma and lung cancer by both IP and oral administration. These studies establish 1,4-dioxohexahydro-6*H*-3,8a-epidithiopyrrolo[1,2-*a*]pyrazine **3c** and related structures as promising clinical candidates for cancer chemotherapy.

## Acknowledgements

Partial financial support for chemical synthesis investigations was provided by the National Institute of General Medical Sciences of NIH (R01GM-30859 to L.E.O.). Biological investigations at the City of Hope were supported in part by NIH P30-CA22572 (to D.H.) and the Drug Discovery and Structural Biology Core facility. Support from the A. Gary Anderson Family Foundation and Panda Charitable Foundation (to D.H.) is gratefully acknowledged. M.B. thanks the Alexander von Humboldt Foundation for a Feodor Lynen Postdoctoral Fellowship, A.P.D. the German Academic Exchange Service (DAAD) for a postdoctoral fellowship, B.M.L. the National Cancer Institute for partial support from postdoctoral fellowship (1F32CA180741), and M.C.W. the National Science Foundation for a graduate fellowship (DGE-1321846). NMR and mass spectra were determined at UC Irvine using instruments purchased with the assistance of NSF and NIH shared instrumentation grants. The authors thank Dr Joseph Ziller and Dr John Greaves, Department of Chemistry, UC Irvine, for their assistance with X-ray and mass spectrometric analyses.

## Notes and references

† At 60% conversion of the cycloadduct, mass spectrometric analysis indicated that a 3 : 2 ratio of mono to dihydroxylated products was present.

§ The relative configuration of the C7 hydrogens was established by <sup>1</sup>H NMR NOE studies.

¶ Conformer populations were generated by molecular mechanics and low energy conformations were optimized by DFT calculations at the B3LYP/631-G\* level. Calculations were done using Spartan 14 (Wavefunction, Inc.).

|| See ESI for details.

\*\* The yield for the other diastereomer was 42%.

- For reviews, see: (a) P. Waring, R. D. Eichner and A. Müllbacher, *Med. Res. Rev.*, 1988, **8**, 499; (b) D. M. Vigushin, N. Mirsaidi, G. Brooke, C. Sun, P. Pace, L. Inman, C. J. Moody and R. C. Coombes, *Med. Oncol.*, 2004, **21**, 21; (c) D. M. Gardiner, P. Waring and B. J. Howlett, *Microbiology*, 2005, **151**, 1021; (d) C.-S. Jiang and Y.-W. Guo, *Mini-Rev. Med. Chem.*, 2011, **11**, 728; (e) E. Iwasa, Y. Hamashima and M. Sodeoka, *Isr. J. Chem.*, 2011, **51**, 420; (f) C.-S. Jiang, W. E. G. Müller, H. C. Schröder and Y.-W. Guo, *Chem. Rev.*, 2012, **112**, 2179.
- B. Onnis, A. Rapisarda and G. Melillo, *J. Cell. Mol. Med.*, 2009, **13**, 2780.



- 3 (a) T. Saito, Y. Suzuki, K. Koyama, S. Natori, Y. Iitaka and T. Kinoshita, *Chem. Pharm. Bull.*, 1988, **36**, 1942; (b) K. M. Cook, S. T. Hilton, J. Mecinović, W. B. Motherwell, W. D. Figg and C. J. Schofield, *J. Biol. Chem.*, 2009, **284**, 26831; (c) Y. Teng, K. Iuchi, E. Iwasa, S. Fujishiro, Y. Hamashima, K. Dodo and M. Sodeoka, *Bioorg. Med. Chem. Lett.*, 2010, **20**, 5085; (d) C. R. Isham, J. D. Tibodeau, A. R. Bossou, J. R. Merchan and K. C. Bible, *Br. J. Cancer*, 2012, **106**, 314; (e) H. T. Tran, H. N. Kim, I. K. Lee, T. N. Nguyen-Pham, J. S. Ahn, Y. K. Kim, J. J. Lee, K. S. Park, H. Kook and H. J. Kim, *J. Korean Med. Sci.*, 2013, **28**, 237.
- 4 (a) C. R. Isham, J. D. Tibodeau, W. Jin, R. Xu, M. M. Timm and K. C. Bible, *Blood*, 2007, **109**, 2579; (b) K. C. Bible, C. R. Isham, R. Xu and J. D. Tibodeau, *Methods and Compositions for Treating Cancer*, *PCT Int. Appl.*, 2008, WO 2008112014 A1 20080918; (c) H. Chaib, A. Nebbioso, T. Prebet, R. Castellano, S. Garbit, A. Restouin, N. Vey, L. Altucci and Y. Collette, *Leukemia*, 2012, **26**, 662; (d) K. M. Reece, E. D. Richardson, K. M. Cook, T. J. Campbell, S. T. Pisle, A. J. Holly, D. J. Venzon, D. J. Liewehr, C. H. Chau, D. K. Price and W. D. Figg, *Mol. Cancer*, 2014, **13**, 91; (e) T. Chiba, T. Saito, K. Yuki, Y. Zen, S. Koide, N. Kanogawa, T. Motoyama, S. Ogasawara, E. Suzuki, Y. Ooka, A. Tawada, M. Otsuka, M. Miyazaki, A. Iwama and O. Yokosuka, *Int. J. Cancer*, 2015, **136**, 289.
- 5 (a) D. Greiner, T. Bonaldi, R. Eskeland, E. Roemer and A. Imhof, *Nat. Chem. Biol.*, 2005, **1**, 143; (b) J. D. Tibodeau, L. M. Benson, C. R. Isham, W. G. Owen and K. C. Bible, *Antioxid. Redox Signaling*, 2009, **11**, 1097; (c) E. Iwasa, Y. Hamashima, S. Fujishiro, E. Higuchi, A. Ito, M. Yoshida and M. Sodeoka, *J. Am. Chem. Soc.*, 2010, **132**, 4078; (d) M. Sodeoka, K. Dodo, Y. Teng, K. Iuchi, Y. Hamashima, E. Iwasa and S. Fujishiro, *Pure Appl. Chem.*, 2012, **84**, 1369; (e) D. Illner, R. Zinner, V. Handtke, J. Rouquette, H. Strickfaden, C. Lanctôt, M. Conrad, A. Seiler, A. Imhof, T. Cremer and M. Cremer, *Exp. Cell Res.*, 2010, **316**, 1662; (f) A. Lakshmikuttyamma, S. A. Scott, J. F. DeCoteau and C. R. Geyer, *Oncogene*, 2010, **29**, 576; (g) Y.-M. Lee, J.-H. Lim, H. Yoon, Y.-S. Chun and J.-W. Park, *Hepatology*, 2011, **53**, 171; (h) C. Dong, Y. Wu, Y. Wang, C. Wang, T. Kang, P. G. Rychahou, Y.-I. Chi, B. M. Evers and B. P. Zhou, *Oncogene*, 2013, **32**, 1351; (i) Y. Yokoyama, M. Hieda, Y. Nishioka, A. Matsumoto, S. Higashi, H. Kimura, H. Yamamoto, M. Mori, S. Matsuura and N. Matsuura, *Cancer Sci.*, 2013, **104**, 889; (j) F. L. Cherblanc, K. L. Chapman, J. Reid, A. J. Borg, S. Sundriyal, L. Alcazar-Fuoli, E. Bignell, M. Demetriades, C. J. Schofield, P. A. DiMaggio Jr, R. Brown and M. J. Fuchter, *J. Med. Chem.*, 2013, **56**, 8616; (k) D. Dixit, R. Ghildiyal, N. P. Anto and E. Sen, *Cell Death Dis.*, 2014, **5**, e1212; (l) M.-C. Lee, Y.-Y. Kuo, W.-C. Chou, H.-A. Hou, M. Hsiao and H.-F. Tien, *J. Leukocyte Biol.*, 2014, **95**, 105.
- 6 (a) K. M. Block, H. Wang, L. Z. Szabó, N. W. Polaske, L. K. Henchey, R. Dubey, S. Kushal, C. F. László, J. Makhoul, Z. Song, E. J. Meuliet and B. Z. Olenyuk, *J. Am. Chem. Soc.*, 2009, **131**, 18078; (b) S. Fujishiro, K. Dodo, E. Iwasa, Y. Teng, Y. Sohtome, Y. Hamashima, A. Ito, M. Yoshida and M. Sodeoka, *Bioorg. Med. Chem. Lett.*, 2013, **23**, 733; (c) N. Boyer, K. C. Morrison, J. Kim, P. J. Hergenrother and M. Movassaghi, *Chem. Sci.*, 2013, **4**, 1646; (d) J. E. DeLorbe, D. Horne, R. Jove, S. M. Mennen, S. Nam, F.-L. Zhang and L. E. Overman, *J. Am. Chem. Soc.*, 2013, **135**, 4117; (e) R. Dubey, M. D. Levin, L. Z. Szabo, C. F. Laszlo, S. Kushal, J. B. Singh, P. Oh, J. E. Schnitzer and B. Z. Olenyuk, *J. Am. Chem. Soc.*, 2013, **135**, 4537.
- 7 L. E. Overman, M. Baumann, S. Nam, D. Horne, R. Jove, J. Xie and C. Kowolik, Preparation of Epipolythiodioxopiperazine ETP Derivatives for Treatment of Cancer, *PCT Int. Appl.*, 2014, WO 2014066435 A1.
- 8 R. Grigg, J. Kemp and W. J. Warnock, *J. Chem. Soc., Perkin Trans. 1*, 1987, 2275.
- 9 O. Tsuge, S. Kanemasa and M. Yoshioka, *J. Org. Chem.*, 1988, **53**, 1384.
- 10 A. D. Borthwick, *Chem. Rev.*, 2012, **112**, 3641.
- 11 X-ray coordinates were deposited with the Cambridge Crystallographic Data Centre: **3c**: 1061873, **3e**: 1061871, **8e**: 1061870; and **8f**: 1061869.
- 12 (a) J. Kim, J. A. Ashenhurst and M. Movassaghi, *Science*, 2009, **324**, 238; (b) J. Kim and M. Movassaghi, *J. Am. Chem. Soc.*, 2010, **132**, 14376.
- 13 E. Öhler, H. Poisel, F. Tataruch and U. Schmidt, *Chem. Ber.*, 1972, **105**, 635.
- 14 K. C. Nicolaou, D. Giguère, S. Totokotsopoulos and Y.-P. Sun, *Angew. Chem., Int. Ed.*, 2012, **51**, 728.
- 15 (a) J. A. Codelli, A. L. A. Puchlopek and S. E. Reisman, *J. Am. Chem. Soc.*, 2012, **134**, 1930; (b) The formation of small amounts of the disulfide and trisulfide products in addition to the predominant tetrasulfide has been noted, see: K. C. Nicolaou, M. Lu, S. Totokotsopoulos, P. Heretsch, D. Giguère, Y.-P. Sun, D. Sarlah, T. H. Nguyen, I. C. Wolf, D. F. Smee, C. W. Day, S. Bopp and E. A. Winzeler, *J. Am. Chem. Soc.*, 2012, **134**, 17320.

